Pseudofunction method: Application to a monolayer of CO and to the Si(111) surface

R. V. Kasowski
Central Research and Development Department, E.I. du Pont de Nemours and Company, Experimental Station, Wilmington, Delaware 19898

M. -H. Tsai, T. N. Rhodin, and D. D. Chambliss
Department of Applied and Engineering Physics, Cornell University, Ithaca, New York 14853-2501
(Received 26 February 1986)

The newly developed pseudofunction method has been developed to provide *ab initio* energy bands and binding-energy curves for molecules, surfaces, and bulk. The effectiveness of this approach is demonstrated by computing the electronic properties of a CO molecule in a monolayer configuration. We find the CO bond length, dipole moment derivative, and the vibrational frequency are close to that of a free CO molecule. We have further demonstrated this new method by computing the surface relaxation of a Si(111)(1×1) four-layer film with one surface saturated by H. The unsaturated surface relaxes inwards by 0.086 Å with a vibrational excitation of 0.038 eV, nearly identical to generalized-valence-bond cluster calculations.

I. INTRODUCTION

Study of the formation of ordered adsorbate monolayers on single-crystal metal surfaces provides a very fruitful approach for the clarification of the physics and chemistry of adsorbate-adsorbate and adsorbate-substrate interactions characteristic of chemisorption on surfaces. Major advances have been achieved in the application of theory to experiment for surface geometry and electronic structure for long-ranged-ordered atomic adsorbates on well-defined surfaces of transition metals. In spite of the great theoretical and practical interest in *molecular-adsorbate* chemisorption systems, equivalent analytical interpretations for ordered molecular-adsorbate monolayers existing either in isolation or on a substrate have been greatly hampered by the limited applicability of available first-principles calculations to relatively large unit-cell systems and to short bond lengths as found in molecules. We present here a study of the isolated monolayer of molecules. These new results are obtained by the use of a new calculational approach capable of providing detailed information on structure and chemical behavior of a molecular-adsorbate monolayer.

Computation of the precise electronic structure and total energy of ordered molecular-adsorbate monolayers is an important objective. *Ab initio* cluster calculations[1,2] have been effectively applied to the interpretation of clean and chemisorbed systems where long-range-order contributions are minimal and the required cluster size is not excessive. In comparison, *ab initio* linearized augmented-plane-wave (LAPW)[3,4] band-structure calculations include long-range-order effects but encounter difficulty in handling the relatively large unit cells and small bond lengths characteristic of molecular adsorbates because of computer effort constraints. This problem arises in part because the size of the wave-function basis is proportional to the inverse of the muffin-tin radius (~ 1.0 a.u. for a CO molecule); thus diagonalization of the Hamiltonian matrix becomes computationally formidable.

Analysis of the electron band structure and atomic geometry of ordered chemisorbed monolayers on single-crystal transition-metal surfaces, particularly CO on Ni(001),[5,6] is often employed as a test case for comparison between theory and experiment. As a first step in studying chemisorption of CO on single-crystal transition metals to this end, we have performed *ab initio* calculations of the CO bond length and vibrational frequency of CO in an isolated carbon monoxide monolayer with a molecular spacing and atomic geometry characteristic of the $c(2\times2)$CO-Ni(001) system. In addition, another example of a test application is calculation of relaxation in the unreconstructed surface of Si(111).

Accurate computational modeling of crystal surfaces with adsorbed layers will be a valuable tool in understanding the interactions at these surfaces, and a great deal of effort has gone into devising computational schemes.[1,3,7–10] Kohn and Sham[11] showed that the ground-state properties of a many-electron system can be computed in terms of one-electron solutions to an effective Hamiltonian computed self-consistently. Particularly interesting among these ground-state properties are the total energies for different atom locations and the electronic band structure which relates to experimentally observed photoemission spectra. A useful approximation applicable in many approaches (including the present work) is the local-density approximation (LDA).

We represent here a small-basis computational technique. This approach, which we call the PSF (pseudofunction) method, uses augmented pseudofunctions as its basis, where the pseudofunctions describe the long-range behavior of wave functions away from atomic cores and can be any function smooth enough to be represented as finite Fourier sums. With well-chosen basis functions this approach is capable of excellent accuracy.

The pseudofunction (PSF) method is improved over the extended muffin-tin-orbital (EMTO) method[12] in two im-

portant respects. First, the pseudofunction is defined as the radial solution of the muffin-tin potential in the region near the muffin-tin boundary. The interior region of the muffin-tin is still a linear combination of spherical Bessel functions as before. The tail is chosen as a spherical Neumann function although other functions such as Gaussians or Slater orbitals would be suitable. The advantage of our new pseudofunction is that the wave function has the correct self-consistent shape in the bonding region which is especially important for molecules. Furthermore, the wave function has the desirable property of consisting of overlapping radial solutions of the muffin-tin potential. Our overlap of radial solutions is exact and the first of its kind. In methods such as linear muffin-tin orbital[13] (LMTO) and augmented spherical wave,[14] potentials (not radial wave functions) are overlapped in an approximate manner.

The other improvement over EMTO is that the expansion of the pseudofunction in plane waves (Gaussians or Slater orbitals could also be used) is augmented with radial solutions of the spherical potential. This augmented pseudofunction then becomes our trial basis function.

We find the bond length of CO is 1.138 Å when the molecules are 3.52 Å apart, as would be found for CO on Ni(001) in a $c(2\times2)$ pattern.[5,6] The computed vibrational frequency is 2157 cm^{-1}. The potentials at infinity indicate the O is negatively charged. Values for free CO (Ref. 15) are 1.128 Å for bond length and 2170 cm^{-1} for frequency with a slightly positive O. It has been reported[16] that two other exchange approximations have been found to increase bond lengths only slightly. Thus, we might expect an equilibrium bond length to change only a little when we change from Hedin-Lundquist exchange.[17]

An additional calculation was performed on the (111) surface of Si to test suitability of PSF for semiconductors. Our model of the Si(111) surface consists of a four-layer film of Si with one surface saturated with H atoms. The remaining surface is then allowed to relax. We find a surface relaxation of 0.086 Å and vibrational excitation of 0.038 eV. These results compare closely to those for the generalized valence bond (GVB) method[18] where a Si_4H_9 cluster was used to model the Si(111) surface. The pseudopotential method obtains 0.29 Å (Refs. 19 and 20) for the surface relaxation for the paramagnetic case. The relaxation is 0.20 Å for a spin-polarized pseudopotential calculation. The pseudopotential calculations were done for a superlattice of ten-layer films. It appears the PSF and GVB methods yield very different results from that of the pseudopotential method.

The PSF technique differs from the widely used pseudopotential[10] and LAPW (Refs. 3 and 4) methods in that we use a local basis function, whereas those methods rely on plane waves. For CO we used 3751 plane waves to expand our locally defined pseudofunctions, and 26 901 for the potential. Such a large number is dictated by the extremely localized molecular bond. In recent work,[21,22] those groups have used only about 800 plane waves for the symmetric diatomic molecule Si_2. No bond length computation was reported for Si_2. Furthermore, the Si_2 bond length of 2.25 Å is nearly twice the bond length of CO.

The PSF formalism is presented in Sec. II. Examples of applications for CO and Si are given in Sec. III. Section IV contains a summary of the PSF method and its potential use.

II. THE PSF CALCULATION APPROACH

A. The extended muffin-tin-orbital method

It is necessary to first summarize the EMTO method.[12] The wave function is defined by muffin-tin orbitals:

$$\chi_l(E_1,r,\kappa^2)=\begin{cases} N_l(R_l+\omega_l\dot{R}_l), & r<R_{\rm MT} \\ -K_l, & r>R_{\rm MT}\ . \end{cases} \tag{1}$$

R_l and $\dot{R}_l$ are the radial solution of the muffin-tin (MT) potential and its first energy derivative for energy E_1 that is fitted onto the spherical Neumann function K_l of energy κ^2. N_l and ω_l provide the fitting parameters. A linear combination of these muffin-tin orbitals form Bloch functions which are used as the trial basis set. Two sets of muffin-tin orbitals (MTO's) are defined for each atom. The energy E_1 and tail parameter κ^2 are chosen so that the filled and empty orbitals have adequate variational freedom. Atoms such as Ni are well represented by an s MTO with $\kappa^2<0.0$ and sp^3d^5MTO's with $\kappa^2>0.0$ (10 MTO's/Ni). Atoms such as Si, C, and O required two sets of sp^3 orbitals (8 orbitals/atom). The Hamiltonian matrix element consists of a term over the muffin tin (MT) and an interstitial term (I). The potential is defined as the spherical contribution $V_{\rm MT}(r)$ and the nonspherical $\Delta V(\mathbf{r})$. The matrix element of the Hamiltonian is

$$\begin{aligned} H_{ij}=&\langle\chi_i^{\mathbf{k}}\,|\,-\nabla^2+V_{\rm MT}+\Delta V-E\,|\,\chi_j^{\mathbf{k}}\rangle_{\rm MT} \\ &+\langle\chi_i^{\mathbf{k}}\,|\,-\nabla^2+\Delta V-E\,|\,\chi_j^{\mathbf{k}}\rangle_I\ . \end{aligned} \tag{2}$$

This matrix element is greatly simplified by adding and subtracting a pseudofunction term over the MT region:

$$\langle P_i^{\mathbf{k}}\,|\,\kappa^2+\Delta V-E\,|\,P_j^{\mathbf{k}}\rangle_{\rm MT}\ .$$

We now obtain the EMTO equation, which is

$$\begin{aligned} H_{ij}=&\langle\chi_i^{\mathbf{k}}\,|\,-\nabla^2+V_{\rm MT}+\Delta V-E\,|\,\chi_j^{\mathbf{k}}\rangle_{\rm MT} \\ &-\langle P_i^{\mathbf{k}}\,|\,\kappa^2+V_{\rm MT}+\Delta V-E\,|\,P_j^{\mathbf{k}}\rangle_{\rm MT} \\ &+\langle P_i^{\mathbf{k}}\,|\,\kappa^2+\Delta V-E\,|\,P_j^{\mathbf{k}}\rangle_{\Omega}\ . \end{aligned} \tag{3}$$

Equation (3) holds provided $P_i^{\mathbf{k}}$ is properly defined:

$$P_i(r,\kappa^2)=\begin{cases} J_l+\omega\dfrac{dJ_l}{d\kappa^2}, & r<R_{\rm MT} \\ -K_l, & r>R_{\rm MT}\ . \end{cases} \tag{4}$$

Thus, the pseudofunction matches continuously to the real function at the muffin-tin radius. Since ΔV is at its maximum value at $R_{\rm MT}$, we assume

$$\langle\chi_i^{\mathbf{k}}\,|\,\Delta V\,|\,\chi_j^{\mathbf{k}}\rangle\sim\langle P_i^{\mathbf{k}}\,|\,\Delta V\,|\,P_j^{\mathbf{k}}\rangle\ .$$

We obtain

$$H_{ij}=\langle\chi_i^{\mathbf{k}}\mid -\nabla^2+V_{\mathrm{MT}}-E\mid\chi_j^{\mathbf{k}}\rangle_{\mathrm{MT}} -\langle P_i^{\mathbf{k}}\mid\kappa^2+V_{\mathrm{MT}}-E\mid P_j^{\mathbf{k}}\rangle_{\mathrm{MT}} +\langle P_i^{\mathbf{k}}\mid\kappa^2+\Delta V-E\mid P_j^{\mathbf{k}}\rangle_{\Omega}\ . \quad (5)$$

The terms over the MT's are solved with one-dimensional radial integration. The term over the unit cell, Ω, is solved by expanding the pseudofunction and ΔV in plane waves. To treat an isolated film, the plane-wave expansion of the pseudofunction are fitted at matching planes above and below the film to decaying radial solutions of the potential in vacuum.

The EMTO method[12] has given accuracy equal to that of LAPW (Ref. 23) and pseudopotentials[24] for Si, Ge, and GaAs. EMTO results compare closely to that of LAPW (Ref. 25) for one- and three-layer Ni films. It has also given good energy bands for CO on Ni.[25] Comparisons for CO on Ni have been only to experiment as there have been no other infinite film theoretical results.

B. The pseudofunction method

The PSF method uses the familiar muffin-tin partitioning of space in describing wave functions, charge densities, and potentials. The basis functions used for solving the Hamiltonian are augmented pseudofunctions. A pseudofunction, abbreviated PSF and represented in this paper by P, is a smooth function specifying the basis function in the interstitial region. Each PSF is represented by a sum of a large number of plane waves with coefficients chosen to reflect a simplified form of the wave function as described below. This choice of a plane-wave representation is not essential to the method; expansions in Gaussians and Slater orbitals are also possible. Plane waves are convenient here because of the two-dimensional periodicity of the systems under study and also because the fast Fourier transform (FFT) algorithm[26] and their orthogonality make them easy to deal with.

Within muffin-tin spheres, the pseudofunction is linearly augmented using radial solutions to the spherical potential within the sphere. Up to a specified angular momentum limit $l_{\max}$, radial functions for specific angular momentum projections of the PSF are replaced with a linearized radial solution. Thus, if the angular momentum projections of a given PSF P about an atom τ are

$$P_{lm\tau}(r)=\int Y_{lm}(\theta,\phi)P(r,\theta,\phi)d\Omega\ , \quad (6)$$

then the corresponding true basis function in that sphere will be

$$X(\mathbf{r})=p(\mathbf{r})+\sum_{1\le l_{\max}}[c_{lm}R_l(r)+c'_{lm}\dot{R}_l(r) -P_{lm}(r)]Y_{lm}(\theta,\phi)\ , \quad (7)$$

where R_l is the radial solution at the energy E_l to the spherical potential, $\dot{R}$ is its derivative with respect to energy, and the coefficients c_{lm} and c'_{lm} are chosen for continuity of X and dX/dr at the muffin-tin radius. A similar augmentation is performed in the vacuum regions except that the functions used for augmentation are one-dimensional solutions to the planar-averaged potential with specified momentum parallel to the film ($G_{\|}$) rather than the angular momentum states used in the spheres.

Since the PSF's determine the boundary conditions for augmentation and thus the entire basis set, they must be chosen carefully. Our formalism allows an arbitrary choice for the Fourier coefficients defining the PSF's, which has advantages to be discussed later. We have achieved good results using PSF's defined in terms of an improvement to muffin-tin orbitals (MTO's). These PSF's are, like MTO's, Bloch sums of angular momentum states about particular atomic sites. Given the wave vector κ, the site τ, and the orbital quantum numbers l and m, all that remains is to specify the radial function. An MTO radial function has two parts, a tail outside the muffin-tin radius, and a smooth continuation within. The tail is a function of fixed (positive or negative) kinetic energy, i.e., a spherical Neumann or Hankel function. The continuation in the sphere of an MTO is also based on spherical Bessel functions.

The present PSF's include an improvement that allows them to better represent the true wave functions in the presence of a potential that varies strongly even outside the muffin-tin spheres. The radial function consists of three parts: a tail for $r>R_{\mathrm{out}}$, $R_{\mathrm{out}}>R_{\mathrm{MT}}$, a segment of radial-solution augmentation for $R_{\mathrm{out}}>r>R_{\mathrm{in}}$, and a smooth continuation to the origin (Fig. 1). The radial solution is based on the spherical part of the potential measured to R_{out}, well beyond R_{MT} (and perhaps into spheres of neighboring atoms).

The assumption behind our use of the MTO's is that the potential in the interstitial region can fairly accurately be represented by a constant. This works well for close-packed metals but is inadequate for open structures with covalent bonding such as silicon and an adsorbed layer of CO. The present PSF's account for differences in potential between regions near the atoms, outside the spheres

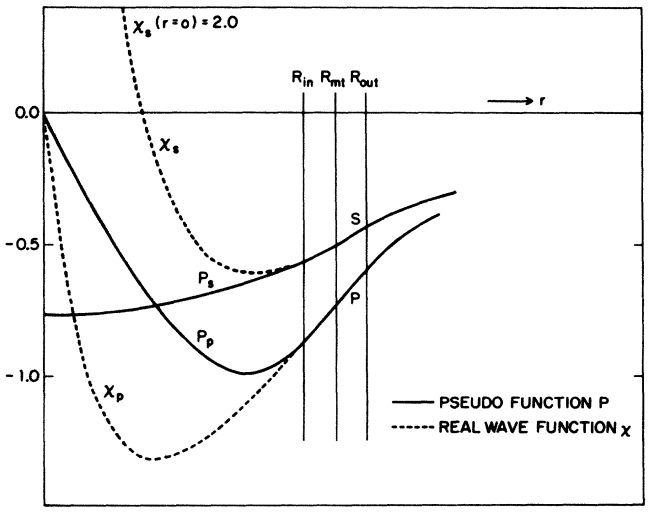

FIG. 1. The pseudofunction (solid curves) is equal to the true radial solution (dashed curve) of the muffin-tin potential in a region about the muffin-tin radius (R_{MT}) defined by R_{in} and R_{out}. The tail is a Neumann function in this particular example although it could be a Slater or Gaussian orbital.

($R_{MT} < r < R_{out}$), and the cavity regions relatively far from any atoms. The assumption of spherical symmetry for the potential is useful as long as R_{out} does not extend far into the strong potential of neighboring atoms. Even a relatively small value for R_{out} of 1.2 R_{MT} gives a substantially more accurate basis function in the binding region roughly between the atoms. We could meaningfully use a larger R_{out} if we solved coupled equations involving nonspherical moments of the potential, but the nonspherical potential is adequately included by variational freedom in combining basis functions from different sites.

Given the basis set, the Hamiltonian matrix elements are expressed as

$$\langle X \mid H-\varepsilon \mid X' \rangle = (\langle P \mid H-\varepsilon \mid P' \rangle)_{I+MT} \tag{8a}$$

$$+(\langle X \mid H-\varepsilon \mid X' \rangle - \langle P \mid H-\varepsilon \mid P' \rangle)_{MT} \tag{8b}$$

$$+(\langle X \mid H-\varepsilon \mid X' \rangle)_{vacuum} . \tag{8c}$$

Note that the kinetic-energy operator in the Hamiltonian is not Hermitian if it is simply truncated at finite boundaries, as in the restriction to the MT spheres, but since the basis functions are smooth at the boundaries the surface terms will vanish provided the same convention is used in applying the operator (only the ket function is differentiated). Equation (8a) is the matrix element of the total Hamiltonian within the slab, evaluated between PSF's. As the PSF's are superpositions of plane waves this amounts to just the convolution of Fourier series; these are evaluated using FFT methods that are fast yet exact.

Equation (8b) is the correction due to augmentation within muffin-tin spheres. These terms are computed using radial integrals. The computation is further simplified if the approximation is made that

$$\langle X \mid V_{nonspher} \mid X' \rangle \simeq \langle P \mid V_{nonspher} \mid P' \rangle , \tag{9}$$

i.e., that nonspherical terms in the potential are evaluated using the PSF rather than the augmentation. In this approximation the Hamiltonian in (8b) has spherical symmetry, so no mixing of terms of different angular momentum occurs in Eq. (8b). For the PSF's as presented defined this is a good approximation because the nonspherical potential is large only near the muffin-tin sphere, where the PSF approximates well the true wave function. For the central atom of a given PSF the agreement from R_{in} to R_{MT} is as good as the Fourier series will allow. At noncentral sites the agreement is acceptable because of smooth matching at the sphere. The error is reduced further because at noncentral atoms the absolute magnitude of the basis function is smaller than at its central site. This approximation, used for the present results, can be eliminated if the need arises.

The final term (8c) represents the correction due to the augmentation in the vacuum. Here again the simplifying assumption is made that the nonsymmetric potential can be neglected; i.e., only the planar-averaged potential is used. It would be fairly easy to include also variations in the potential parallel to the slab.

The Hamiltonian matrix is computed and diagonalized for each sampled point of the irreducible sector of the surface Brillouin zone; the charge density is then computed from the occupied states:

$$\rho_{tot} = \sum_{\text{occupied } \lambda} \left| \sum_i \gamma_{\lambda i} X_i(\mathbf{r}) \right|^2 = \rho_{PSF} + \sum_\tau \rho_{RW,\tau} + \rho_{vac} . \tag{10}$$

The first term gives a plane-wave expansion of the charge density due to the PSF's. The third term is the vacuum charge density. The second term is the correction for the difference between PSF's and their true basis functions; again the approximation is made that the nonspherical terms in this correction are negligible. The justification for this is that the nonspherical terms must vanish near the origin while the correction itself vanishes at the muffin-tin sphere. However, these nonspherical terms can be calculated in terms of multipole charge densities, from which their multipole potentials can be easily obtained by simple radial integrations. Associated with each atom, τ, we added and subtract two charge densities. One is a point charge q_τ and another is a Gaussian charge density $\rho_{G,\tau}$. The total system charge density ρ as a sum of the valence electronic charge density ρ_{tot}, and the charge of the ion core z_τ is then given by

$$\rho = \sum_\tau \rho_\tau + \sum_\tau \rho_{F,\tau} + \rho_{PWV} , \tag{11}$$

where

$$\rho_\tau = \rho_{RW,\tau} - q_\tau \delta(\mathbf{r}_\tau) , \tag{12}$$

$$\rho_{F,\tau} = (Z_\tau + q_\tau)\delta(\mathbf{r}_\tau) - \rho_{G,\tau} , \tag{13}$$

$$\rho_{PWV} = \rho_{PSF} + \sum_\tau \rho_{G,\tau} + \rho_{vac} . \tag{14}$$

$\mathbf{r}_\tau$ is the position vector relative to the nucleus of the atom and $\delta(\mathbf{r}_\tau)$ is the three-dimensional delta function. The q_τ is chosen such that ρ_τ is neutral within each muffin-tin sphere, i.e., q_τ is equal to the total charge of $\rho_{RW,\tau}$ in magnitude but opposite in sign. The $\rho_{G,\tau}$ is chosen such that its total charge is equal to $-(Z_\tau + q_\tau)$. With these q_τ and $\rho_{G,\tau}$, ρ_τ, $\rho_{F,\tau}$, and ρ_{PWV} have zero not charge separately. The total Coulomb potential is a superposition of the potentials resulting from these three charge densities.

$\rho_{G,\tau}$ in Eq. (14) is expanded in plane waves. The Coulomb potential given rise by the neutral ρ_{PWV} is solved using the Green-function method. The potentials due to ρ_τ are obtained by radial integrations. Since ρ_τ is neutral within the MT sphere, this potential is zero outside the sphere. The Coulomb potential $V_{F,\tau}(r_\tau)$, due to the charge density $\rho_{F,\tau}$ is simply

$$V_{F,\tau}(r_\tau) = 2(Z_\tau + q_\tau)\text{erfc}(\eta r_\tau)/r_\tau \text{ Ry} , \tag{15}$$

where $\text{erfc}(\eta r_\tau)$ is the complementary error function, η is the decaying parameter in the Gaussian charge density, and r_τ is the radial distance from the nucleus of atom τ. η, r_τ, Z_τ, and q_τ are in atomic units. The LAPW method uses the same technique by adding and subtracting Gaussian charge densities. However, unlike the LAPW method, we do not confine the Gaussian charge

density within the muffin-tin sphere. Rather, we let it extend up to the vacuum boundaries. This feature is particularly important in the molecular-adsorbate system. Due to the smallness of the muffin-tin spheres in the adsorbate, a relaxed Gaussian charge density is desired to have a satisfactory convergence in the plane-wave expansion.

The exchange-correlation potential is computed using the local-density approximation, within the formulation of Hedin and Lundquist.[17] This is done by evaluating the total charge density (including core states), and it's exchange-correlation potential V_{xc} on a grid of space. The result is added to the plane-wave expansion of the potential.

For computation of the basis set it is necessary to know the spherical parts of the potential about each atom both for finding the PSF in the region $R_{in} < r < R_{out}$ and for computing the augmentations. The spherical projections out to R_{MT} of the plane-wave potential are therefore added to the muffin-tin radial potential and subtracted from the plane-wave potential, leaving the total potential unchanged but making available the true spherical parts. The spherical projections beyond R_{MT} are also computed for defining the PSF's; the radial functions thus computed are not used as part of the total potential in computing matrix elements so these parts need not be subtracted off.

The important feature of the PSF approach is that the basis set, while small, is specified in a parameter space large enough that very close representation of true wave functions are accessible. The accuracy of this method is determined by the choice of basis. If the basis could be chosen ideally, the method would give the accuracy of complete-basis methods such as LAPW. With the PSF method, it is possible to work with any desired basis, including Gaussians, Slater orbitals, and MTO's in any combination, and to enlarge the basis when more accuracy is needed. More importantly, it is possible to evaluate quantitatively the appropriateness of these particular basis. This is necessary for studies of large systems beyond the present reach of LAPW and other highly accurate methods; for these systems variational freedom must be replaced by scientific judgment to achieve high accuracy.

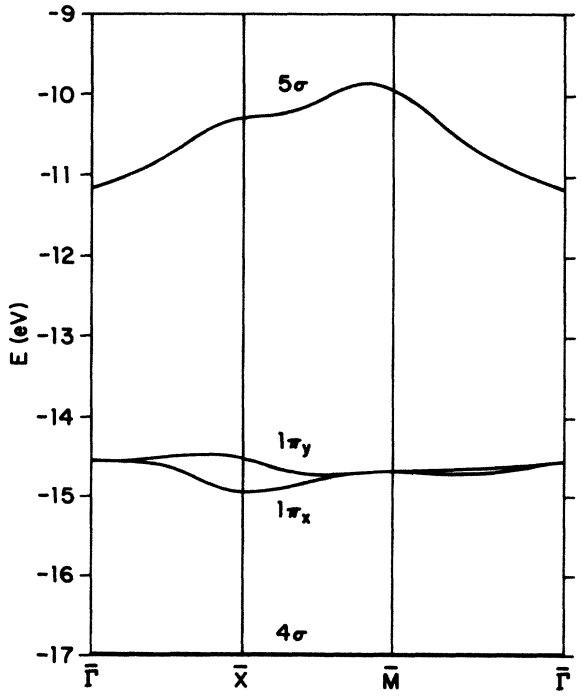

FIG. 2. The energy bands of an isolated CO monolayer.

It should be noted that while the PSF method is presented here in terms of application to thin films, it can be applied as well to isolated molecules, polymers, and clusters, true surfaces, bulk-bulk interfaces, and of course bulk behavior. For molecules and clusters the vacuum augmentation is changed from a one-dimensional augmentation at a planar boundary to a radial augmentation at a spherical surface. The plane-wave expansion can still be used for PSF's with some modifications, although for nonperiodic structures the plane waves lose their special appropriateness, and it may be more convenient to expand using Gaussian or Slater orbitals. For true surfaces and bulk-bulk interfaces, the vacuum is replaced by bulk on one or both sides. This embedding can be accounted for in the calculation with an effective potential determined by the Green's function for the bulk.

III. EXAMPLES OF APPLICATION FOR CO MONOLAYER AND FOR Si(111)

A. C—O bond length determination for monolayer of CO

CO is known to chemisorb onto a Ni(001) crystalline surface in an ordered $c(2\times2)$ pattern.[5,6] We have computed the structural and electronic properties of CO in a monolayer configuration. The molecules are 3.52 Å apart as they would be for CO on Ni.

Our basis set consists of only 14 functions. On both the C and O, we have sp^3 functions with a spherical Neumann function tail that is decaying ($\kappa^2=-0.3$ Ry) and P^3 functions with oscillating tail ($\kappa^2=0.5$ Ry). The planes above and below the film are placed at ±4.5 a.u. relative to the center of the film. It is easy to converge our total-energy values to 0.0001 Ry as a monolayer of CO is a wide-band-gap material.

In Fig. 2, the energy bands for the monolayer of CO are plotted. In this figure, the zero energy is defined at the infinity above the O atom. The 5σ band has a bandwidth about 1.2 eV, and is about 6 eV above the 4σ band. 1π is split at the $\bar{X}$ point by 0.5 eV. The separation between 1π and 4σ is about 2.4 eV; this is reduced substantially from that of free CO, 2.8 eV. The 4σ band is nearly a straight line. The substantial 1π and 5σ bandwidths reflect a significant influence of the long-range order and the CO-CO coupling. In Fig. 3, the total energy is plotted as a function of bond length. We obtain an equilibrium bond length of 1.138 Å and a vibrational frequency of 2157 cm^{-1}. These values are remarkably similar to that of free CO, namely 1.128 Å for the bond length and 2170 cm^{-1} for the vibrational frequency.

An infinite dipole layer gives rise to an electrostatic potential difference on the two sides of the layer. The relation between the potential difference and the dipole densi-

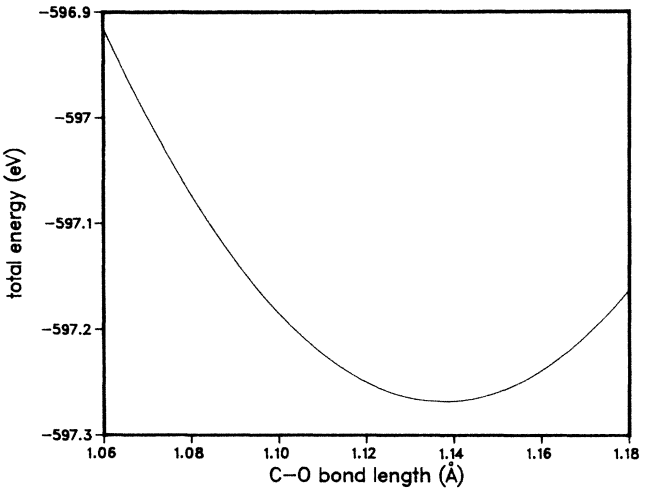

FIG. 3. Potential energy curve for the CO monolayer.

ty is given by $\Delta\phi = 37.7D$, where $\Delta\phi$ is the potential difference in volts and D is the dipole density in debye/Å^2. In our system of monolayer of CO, $\Delta\phi$ corresponds to the Coulomb potential difference between $z = +\infty$ and $-\infty$. Thus the net dipole, μ in debye, of a CO molecule can be calculated by

$$\mu = 0.361137VA \ , \tag{16}$$

where A is the surface area of a unit cell in Å^2 and V is the potential (energy) difference in Ry.

The Coulomb potential above the O atom at infinity is 0.23 Ry, relative to that above the C atom for the equilibrium C—O bond length. It corresponds to a net dipole moment of -1.0 debyes for a CO molecule; the negative sign stands for a C^+O^- dipole. The dipole moment as a function of the C-O distance is shown in Fig. 4. The curve is nearly a straight line with a slope of 3.16 debye/Å. This dipole moment derivative is very close to the free CO value of 3.14 debye/Å.[15] The large dipole moment, if using a pair of point charges model separated by 1.14 Å, corresponds to a charge of $0.2e$. That is, there are about 0.2 electrons shifted from the C atom to the O atom. Since the O atom is more electronegative than the C atoms, a small charge shift resulting from the CO-CO coupling is reasonable. It has been shown that the small free CO dipole moment results from detailed balancing between a triple-bond CO, with a C^-O^+ dipole, and a single-bond CO, with a C^+O^- dipole.[27] The single bond is favored for a longer bond length. Our slightly larger bond length and a C^+O^- dipole are consistent with this picture. Besides, the CO-CO coupling in the monolayer should draw some charge from the C-O bonding region, which reduces the population of the triple-bond CO.

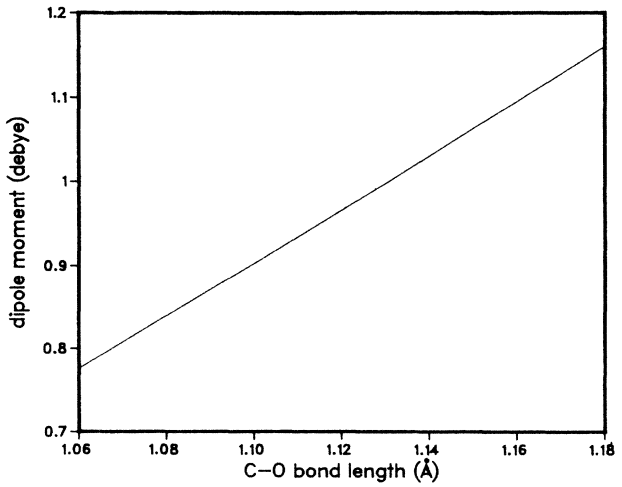

FIG. 4. Dipole moment of CO as a function of C-O distance.

In this CO monolayer calculation we choose the wave vector of the plane waves up to $G_x^{\max} = G_y^{\max} \sim 5/R_{\mathrm{MT}}$ and $G_z^{\max} \sim 7/R_{\mathrm{MT}}$ for the expansion of the PSF's. $G^{\max}$'s are doubled for the expansion of the potential. LAPW method uses a $G^{\max}R_{\mathrm{MT}} \sim 7$ criterion for its choice of the plane-wave basis set for transition-metal systems. The number 7 is chosen from the first root of the spherical Bessel function with $l = 2$. Since we have system dominated by s and p orbitals, we can reduce the criterion to the first root of the $l = 1$ spherical Bessel function, which is close to 5. We have tested several sets of plane waves and find that the dipole moment is very sensitive to the number of plane waves when it is insufficient. For instance, when $G_x^{\max} = G_y^{\max} = G_z^{\max} \sim 2.8/R_{\mathrm{MT}}$ is used, the dipole moment becomes only about one-half the value given previously. The dipole moment even changes sign to that of free CO when the number of plane waves is reduced further.

We have also tested a double layer of CO with the two C atoms facing each other and separated by 7.12 and 4.2 Å. This is an inversion symmetric system. Figure 5

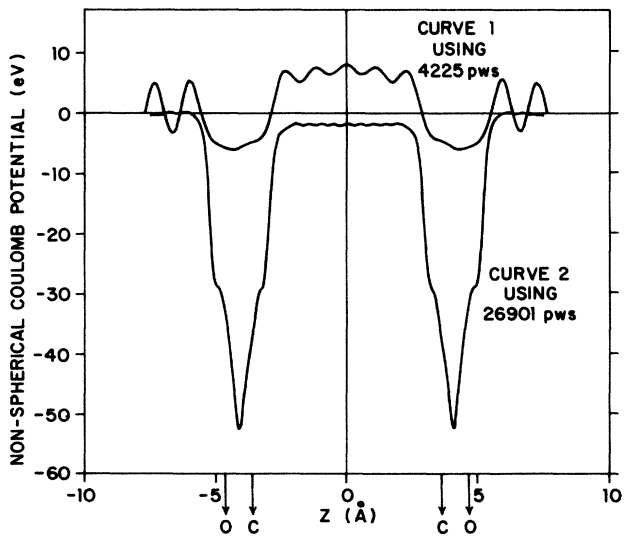

FIG. 5. The nonspherical Coulomb potential along the molecular axis of a double layer of CO separated by 7.12 Å. Dashed curve uses 4225 plane waves, while the solid curve uses 26 901 plane waves.

shows the nonspherical Coulomb potential along the common molecular axis with a 7.12 Å C-C separation. The dashed curve uses $G_x^{\max}=G_y^{\max}\sim 2.8/R_{\mathrm{MT}}$ and $G_z^{\max}\sim 1.4/R_{\mathrm{MT}}$ and the solid curve uses $G_x^{\max}=G_y^{\max}\sim 2.8/R_{\mathrm{MT}}$ and $G_z^{\max}\sim 2.8/R_{\mathrm{MT}}$. It is clear that the potential is poorly represented by the smaller set of plane waves. Even the larger set still has a wavylike plateau in between the layers. The depth of this plateau results from the net dipole density in either one of the CO layers. A negative plateau corresponds to a C^+O^- dipole. Figure 5 demonstrates that a large enough number of plane waves is essential to yield a correct film dipole moment. The dipole moment obtained from the double-layer calculations is similar to that of the monolayer; this seems to indicate that the large dipole moment we obtained is not an artifact.

In summary, the application of our PSF method on the monolayer of CO yields very similar equilibrium bond length, dipole moment derivative, and vibrational frequency to that of free CO. These properties are related to changes in the normal direction, which should depend mostly on the short-range C—O bonding and are not expected to change significantly by the long-range ordering and CO-CO coupling. On the other hand, the electronic structures and the dipole moment do change substantially from free CO values. The large C^+O^- dipole moment is explainable as a depopulation of the triple bond, $C^-\equiv O^+$, due to CO-CO coupling so that the balancing between the triple bond and the single bond, C^+—O^- in free CO, is shifted to favor the single bond.

B. Relaxation of (111) surface of Si

We have chosen to model the (111) surface of Si with a four-layer film with the dangling bonds on one side saturated with H atoms. The remaining surface is then relaxed to find the equilibrium. Our model differs from that used in pseudopotential calculations,[19,20] where a superlattice of ten-layer films was used and both sides of the film were relaxed symmetrically. Such a model must be chosen carefully to avoid interactions of dangling bonds between neighboring films and across the film.

The binding-energy curve for relaxation of the surface layer is shown in Fig. 6. The surface layer relaxes inwards by 0.086 Å. The corresponding vibrational excitation is 0.038 eV. The potential at infinity above the H saturated surface is −0.07 Ry, relative to the potential being 0.0 above the relaxed surface. Thus, termination of dangling bands with H is an appreciable effect. Different results might thus be expected from having films with no H termination on one side as in a superlattice.

Our results are in remarkable agreement with the GVB (Ref. 18) method for a cluster. Redondo *et al.*[18] modeled the (111) surface of Si with one Si above a triad of Si atoms. The dangling bonds of the triad are saturated by nine H atoms. They obtain 0.08 Å for the relaxation and 0.036 eV for the vibrational excitation.

The pseudopotential method[19,20] obtains very different results for a superlattice of ten-layer films. The relaxation is 0.29 Å or 0.26 Å. We estimate from this work a vibrational excitation of about 0.032 eV. With spin polarization, the relaxation is reduced to about 0.20 Å.[19] The difference in relaxation of 0.26 versus 0.29 is probably due to calculational setup.

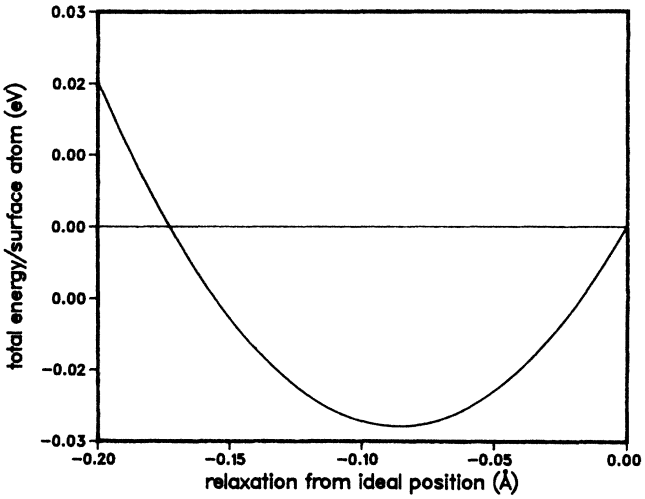

FIG. 6. Potential-energy curve for relaxation of one surface of Si(111) with the other surface saturated with H.

Thus, the PSF results for a film with one surface saturated with H is more similar to a GVB cluster than to that of a superlattice with no H saturation on either surface. It will be important to investigate the various reconstruction models of the Si(111)-(2×1) surface. The superlattice pseudopotential results strongly favor the Pandey[20] covalently π-bonded chain model of the surface and not the ionic Hanneman model.[28] Low-energy electron diffraction calculations[29] favor the ionic Hanneman model over the Pandey model of the (111)-(2×1) reconstruction.

The energy bands for the Si film are shown in Fig. 7.

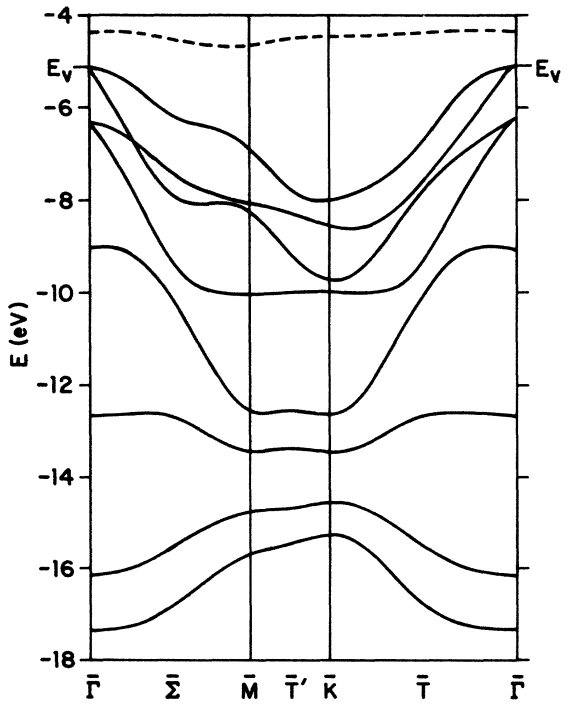

FIG. 7. Energy bands for an unrelaxed four-layer Si(111) with one surface saturated with H atoms.

As expected, there is only one band of dangling bonds in the band gap. A band of derived H states is found at about -12.8 eV. Our dangling bond bands are very similar to that of pseudopotentials when properly translated into the same Brillouin zone. But the electronic states are sufficiently different to give different surface bond lengths.

A plausable explanation for the large difference in results between the superlattice model and our H-saturated model is difference in screening. A semiconductor does not have a source of electrons to screen out long-range interaction as metals do. Therefore, the dangling bonds at one surface see different long-range forces depending on whether the other surface is H saturated and semiconducting or whether it is unsaturated and metallic as in the superlattice. Thus, it will be important to make comparisons to experiment to determine which model is a more accurate reflection of the semi-infinite solid.

IV. SUMMARY AND FUTURE POTENTIAL USE

The PSF method has been shown to give an accurate bond length, dipole moment derivative, and vibrational frequency for CO molecules in a monolayer configuration. We have also computed a surface relaxation of Si(111) in close agreement with cluster calculations using an entirely different method (GVB). The success of the method for these two problems indicates that the method will be useful in studying molecules on surfaces of metals and surfaces of semiconductors. Current calculations underway include CO on Ni to determine whether the top site or the fourfold site is the preferred bonding site. We will also study the preferred (2×1) reconstruction for a Si(111) film with one side saturated by H and compare it to pseudopotential results.

The PSF method is well suited for the study of defects as the method is applicable to either long-range or short-range effects. The small basis set again is of great importance as it enables calculations on large unit cells. Large unit cells allow one to model more accurately the crystalline response to a given defect.

Note added. An alternative to defining two sets of PSF orbitals per atom in the unit cell is to use a mixed basis set. The procedure is similar to the mixed basis approach of Louie.[30] Our basis consists of one set of PSF's per atom along with a small number of augmented plane waves. Preliminary results for films indicates that this is an efficient approach to obtain proper long-range behavior.[31]

ACKNOWLEDGMENTS

Use of computing support and other facilities of the E. I. du Pont Company is gratefully acknowledged, as well as partial support for one of us (M.-H.T.). Support for M.-H.T. from the National Science Foundation Grant No. NSF-DMR-83-03742 is also acknowledged.

[1]C. F. Melius, B. D. Olafson, and W. A. Goddard III, Phys. Rev. Lett. **98**, 457 (1974).
[2]J. C. Slater and K. H. Johnson, Phys. Rev. B **5**, 844 (1972).
[3]O. Jepsen, J. Madsen, and O. K. Andersen, Phys. Rev. B **26**, 2790 (1982).
[4]H. Krakauer, M. Posternak, A. J. Freeman, and D. D. Koelling, Phys. Rev. B **23**, 3859 (1981).
[5]J. C. Bertolini and B. Tardy, Surf. Sci. **102**, 131 (1981); C. L. Allyn, T. Gustafsson, and E. W. Plummer, Solid State Commun. **28**, 85 (1978); R. G. Tobin, S. Chiang, P. A. Thiel, and P. L. Richards, Surf. Sci. **140**, 393 (1984).
[6]M. Passler, A. Ignatiev, F. Jona, D. W. Jepsen, and P. M. Marcus, Phys. Rev. Lett. **43**, 360 (1979). S. Anderson and J. B. Pendry, *ibid.* **43**, 363 (1979).
[7]J. G. Gay, J. R. Smith, and F. J. Arlinghauss, Phys. Rev. Lett. **38**, 561 (1977).
[8]J. Allison and W. A. Goddard III, Surf. Sci. **115**, 553 (1982).
[9]K. Herman, P. S. Bagus, and G. W. Bauschliches, Phys. Rev. B **30**, 7313 (1984).
[10]M. Schlutter, J. R. Chelikowsky, S. G. Louie, and M. L. Cohen, Phys. Rev. B **12**, 4200 (1975).
[11]W. Kohn and L. J. Sham, Phys. Rev. **140**, A1133 (1965).
[12]R. V. Kasowski, Phys. Rev. B **25**, 4189 (1982).
[13]O. K. Andersen, Phys. Rev. B **12**, 3060 (1975).
[14]A. R. Williams, J. Kubler, and C. D. Gelatt, Jr., Phys. Rev. B **19**, 6094 (1979).
[15]C. Chakerian, Jr., J. Chem. Phys. **65**, 4228 (1976).
[16]M. T. Yin and M. L. Cohen, Phys.Rev. B **26**, 5668 (1982).
[17]L. Hedin and B. I. Lundquist, J. Phys. C **4**, 2064 (1971).
[18]A. Redondo, W. A. Goddard III, T. C. McGill, and G. T. Surratt, Solid State Commun. **20**, 733 (1976).
[19]J. E. Northrup, J. Ihm, and M. L. Cohen, Phys. Rev. Lett. **47**, 1910 (1981).
[20]K. C. Pandey, Phys. Rev. Lett. **49**, 223 (1982).
[21]E. Wimmer, H. Krakauer, M. Weinert, and A. J. Freeman, Phys. Rev. B **24**, 864 (1981).
[22]M. Schluter, A. Zunger, G. Kerker, K. M. Ho, and M. L. Cohen, Phys. Rev. Lett. **42**, 540 (1979).
[23]D. R. Hamann, Phys. Rev. Lett. **42**, 662 (1979).
[24]S. G. Louie, K. M. Ho, J. K. Chelikowsky, and M. L. Cohen, Phys. Rev. B **15**, 4527 (1977).
[25]T. N. Rhodin, M. H. Tsai, and R. V. Kasowski, Appl. Surf. Sci. **22/23**, 687 (1985).
[26]C. O. Brigham, *The Fast Fourier Transform* (Prentice-Hall, Englewood Cliffs, NJ, 1974).
[27]W. M. Huo, J. Chem. Phys. **43**, 624 (1965).
[28]D. Hanneman, Phys. Rev. **121**, 1093 (1961).
[29]R. Feder, Solid State Commun. **45**, 51 (1983).
[30]S. G. Louie, K. M. Ho, and M. L. Cohen, Phys. Rev. B **19**, 1774 (1979).
[31]R. V. Kasowski and M. -H. Tsai (unpublished).
[32]D. Hanneman, Phys. Rev. **121**, 1093 (1961).
[33]R. Feder, Solid State Commun. **45**, 51 (1983).
[34]S. G. Louie, K. M. Ho, and M. L. Cohen, Phys. Rev. B **19**, 1774 (1979).
[35]R. V. Kasowski and M. -H. Tsai (unpublished).